Supplementary materials

Effects of hydrostatic pressure on epithelial dome formation and stability

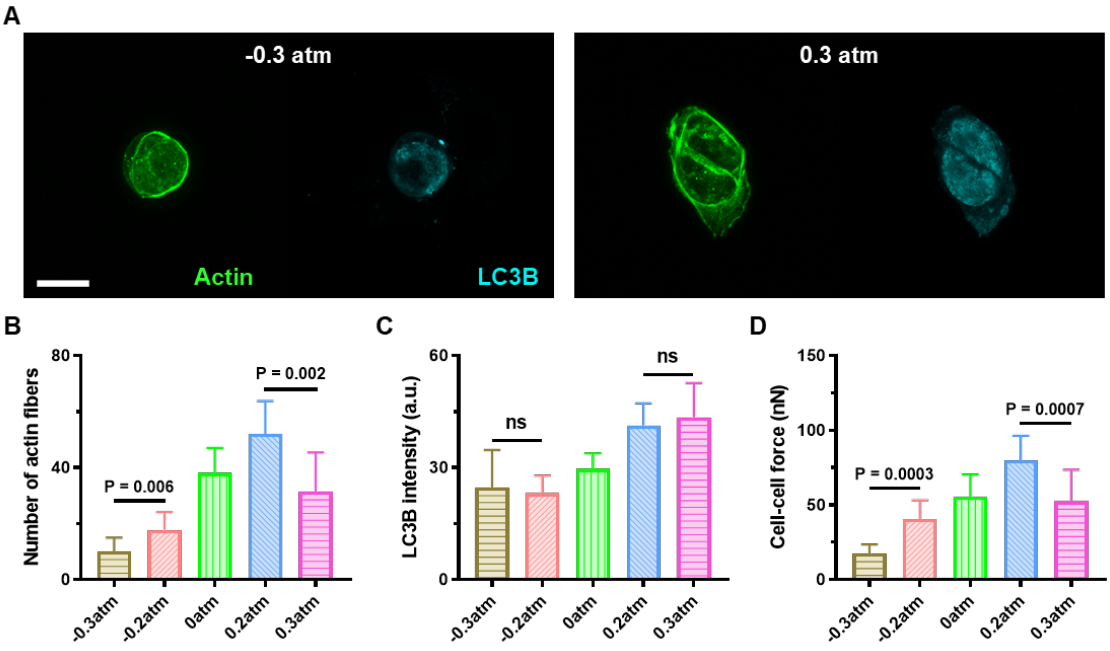

Fig. S1 Effects of hydrostatic pressure on the mechanical properties of paired cells.
(A) Representative fluorescence images of actin (green) and LC3B (turquoise) in paired cells after 12 hours loading of -0.3 atm and 0.3 atm. Scale bar, 20 μm.
(B) Statistical analyses of the number of actin fibers in each group. Among them, the number of fibers was the largest under 0.2 atm and the least under -0.3 atm.
(C) Statistical analyses of LC3B fluorescence intensity in each group. Among them, the fluorescence intensity of LC3B was the highest under 0.3 atm and the lowest under -0.2 atm.
(D) Statistical analyses of cell-cell force in each group. Among them, the force was the largest under 0.2 atm and the least under -0.3 atm.

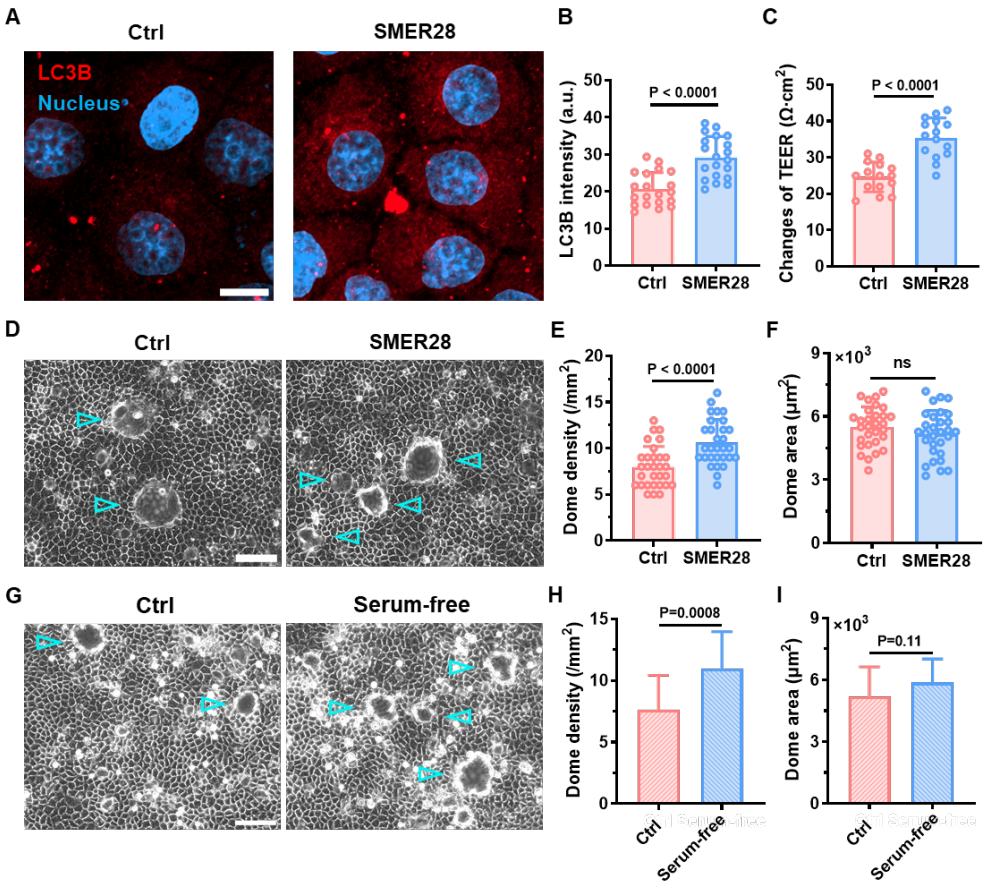

Fig. S2 Effects of cell autophagy on dome formation.

(A) Representative LC3B fluorescence images of monolayers after 12 hours loading of 0 atm without and with SMER28 treatment. Noted that SMER28 is the autophagy enhancer, and the concentration used is 10 μM. Scale bar, 10 μm.

(B) Statistical analysis of the fluorescence intensity of LC3B after 12 hours in each group. It was observed that the addition of autophagy enhancer increased the expression of LC3B in cell monolayers.

(C) Changes of transepithelial electrical resistance (TEER) within 12 hours in each group. It was observed that the addition of autophagy enhancer increased the resistance of cell monolayers.

(D) Phase contrast images of cell monolayers after 12 hours loading of 0 atm without and with SMER28 treatment. Scale bar, 100 μm.

(E) Statistics of the density of domes on cell monolayers after 12 hours in each group. The addition of autophagy enhancers significantly increased the number of domes.

(F) Statistics of the dome area on cell monolayers after 12 hours in each group. The addition of autophagy enhancers had little effect on the dome area.

(G) Phase contrast images of cell monolayers cultured under control (0 atm and standard culture medium) and serum-free DMEM after 12 hours loading of 0 atm. Scale bar, 100 μm.

(H) Statistics of the dome density on cell monolayers under control and serum-free DMEM conditions.

(I) Statistics of dome area on cell monolayers under control and serum-free DMEM conditions.

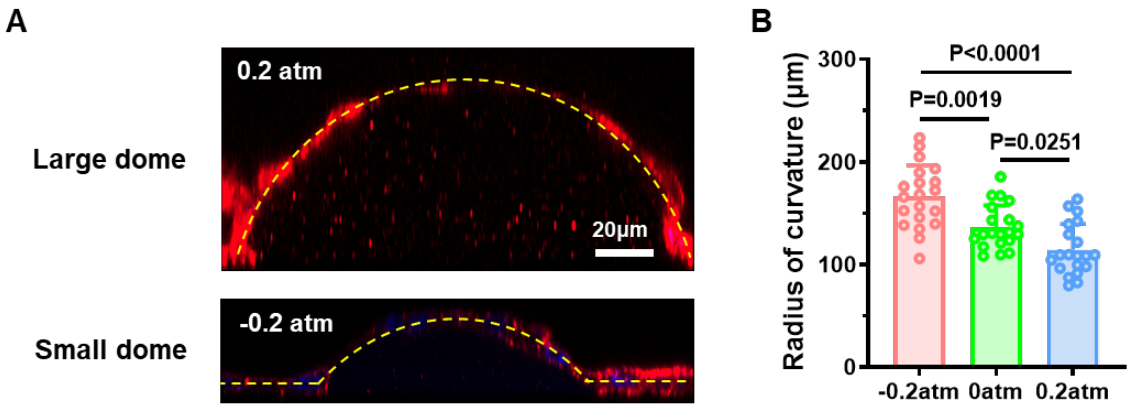

Fig. S3 The effect hydrostatic pressure on the dome dimension and curvature. (A) Fluorescence images of large and small domes, and red represents actin. Scale bar, 20 μm. (B) Statistics of the curvature radius of domes at different hydrostatic pressures.

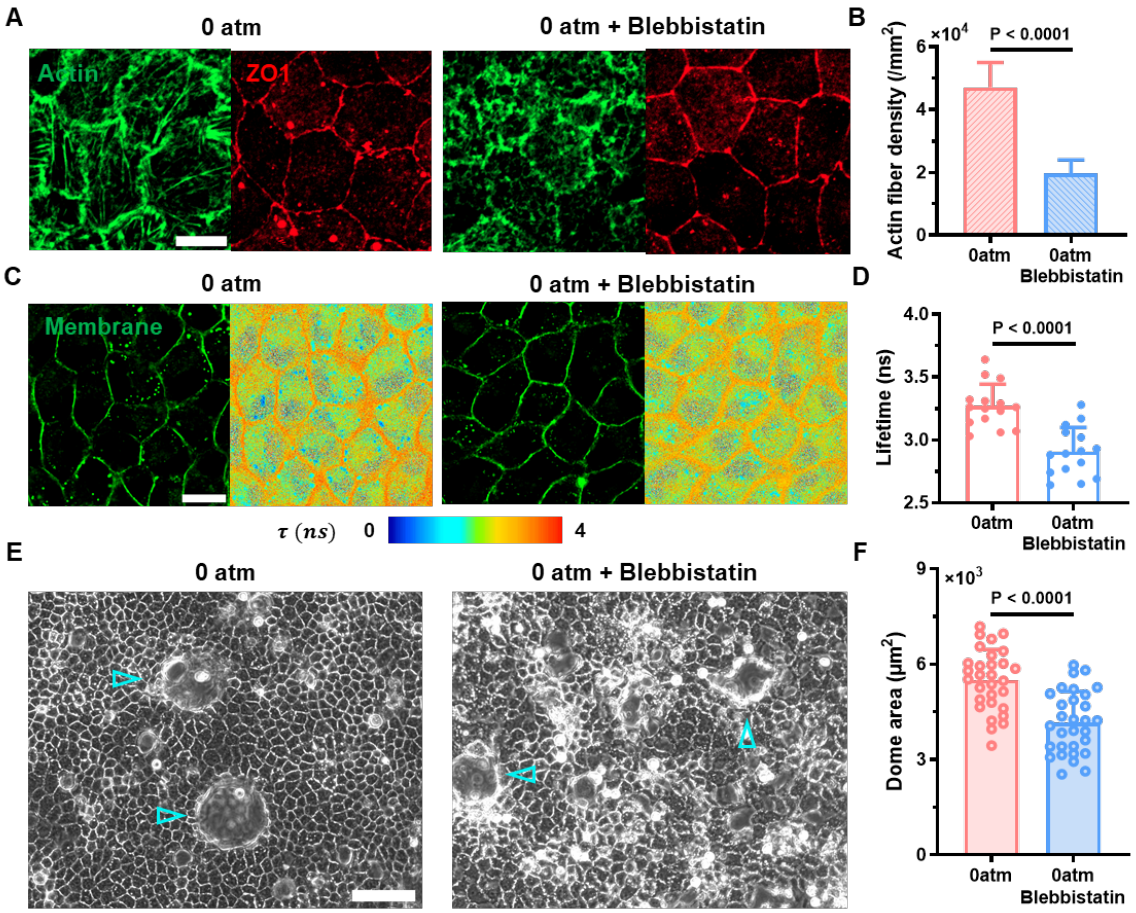

Fig. S4 Effects of actin cytoskeleton contractility on dome formation.

(A) Representative fluorescence images of actin and ZO1 (tight junction protein) in cell monolayers after 12 hours loading of 0 atm without and with blebbistatin treatment. The concentration of blebbistatin is 25 μM. The treatment with blebbistatin did not affect tight junctions. Scale bar, 10 μm.

(B) Statistics of actin fiber density after 12 hours in each group. The treatment with blebbistatin reduced actin fiber density and organization.

(C) Fluorescence and fluorescence lifetime images of the cell membrane after 12 hours loading of 0 atm without and with blebbistatin treatment. Scale bar, 20 μm.

(D) Statistics of fluorescence lifetime of the cell membrane after 12 hours in each group. The inhibition of cell contraction decreased the membrane tension.

(E) Phase contrast images of cell monolayers after 12 hours loading of 0 atm without and with blebbistatin treatment. Scale bar, 100 μm.

(F) Statistics of dome area on cell monolayers after 12 hours in each group. The inhibition of cell contraction decreased the dome area.

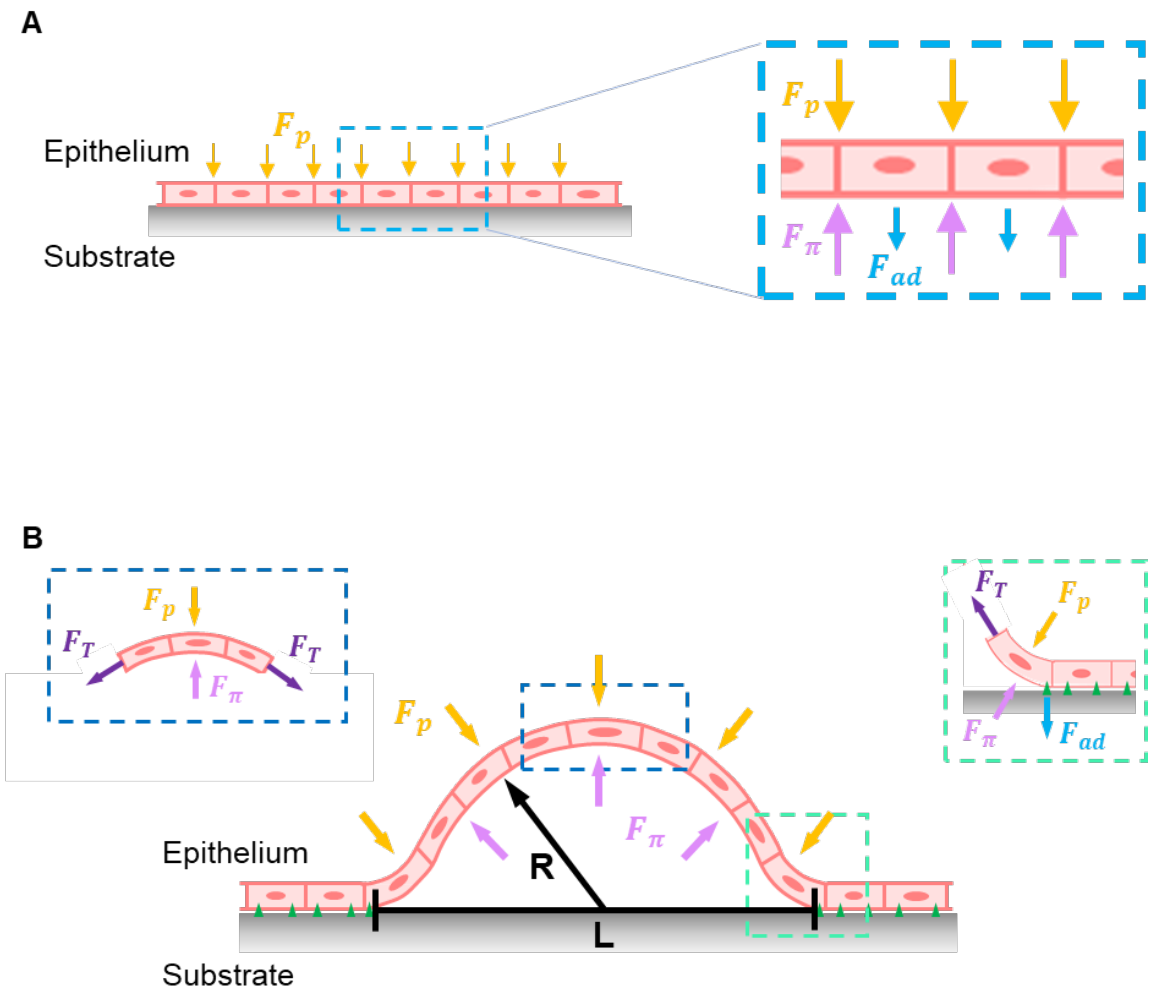

Fig. S5 Schematic diagram of the mechanical forces that control dome formation and expansion. (A) The force-balance diagram for the pre-dome formation state. The external hydrostatic pressure F_P is balanced by the osmotic pressure F_π and adhesion force F_{ad}.

(B) The force-balance diagram for the post-dome formation state. At the edge of the dome, the two pressures (F_P, F_π) are balanced by the membrane tension F_T and the adhesion force F_{ad}. Away from the edge, there is a balance between the two pressures and the membrane tension.

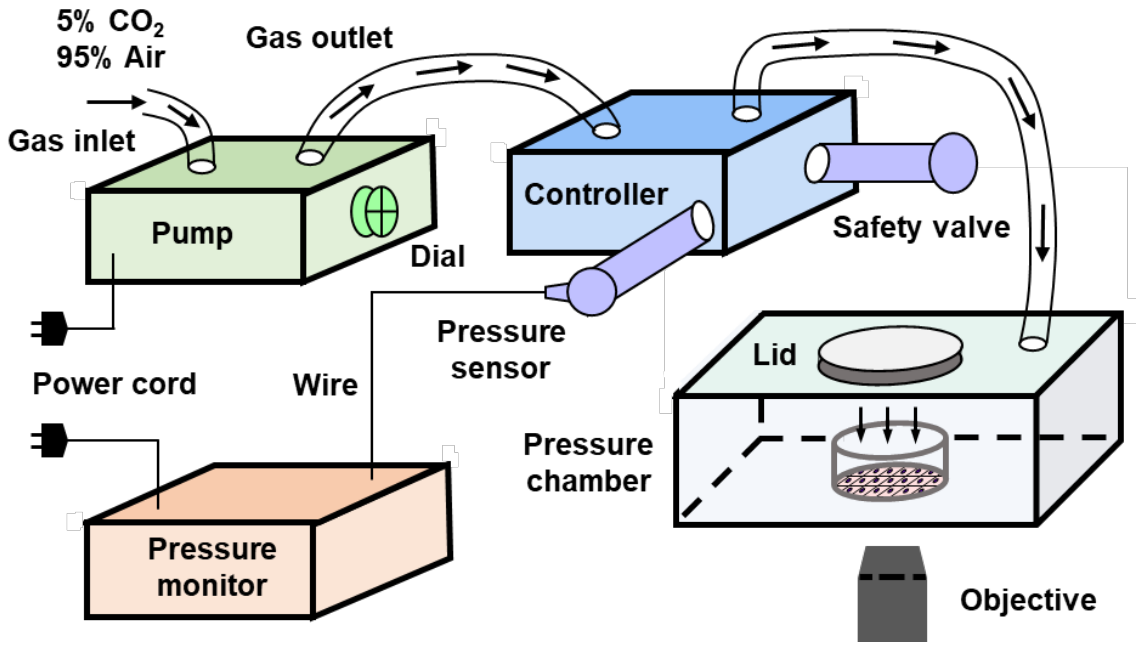

Fig. S6 Schematic diagram of the hydrostatic pressure generator.

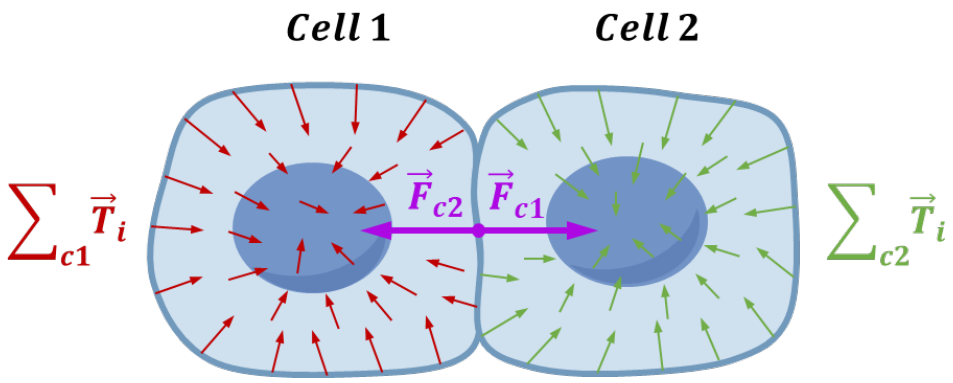

Fig. S7 Schematic diagram of calculating the force between cells using the traction imbalance method. For a given pair of cells, the vector sum of traction force $\sum_{c1} \vec{T_i}$ generated by cell 1 was balanced by the cell-cell force $\vec{F}_{c1}$ exerted on cell 1 by cell 2. Similarly, the vector sum of the traction forces $\sum_{c2} \vec{T_i}$ generated by cell 2 corresponds to the force $\vec{F}_{c2}$ exerted on cell 2 by cell 1.

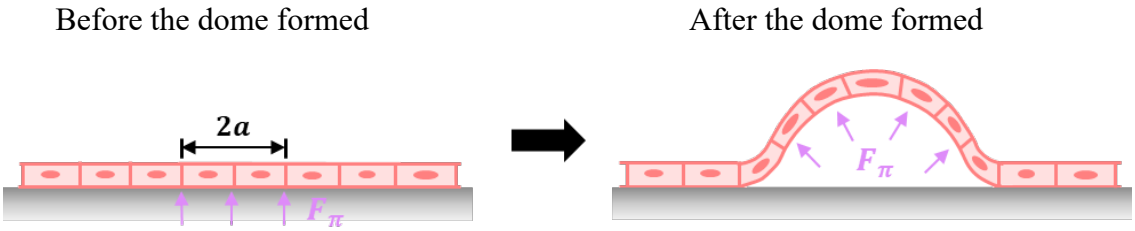

Fig. S8 Schematic diagram illustrating the method of applying osmotic pressure at the initial moment in our numerical simulation.

Numerical simulation

Mechanical model

In the vertex model, the epithelial monolayer can be described by a network of polygons with periodic boundary, and the motions of each cell α are determined by the evolution of the position vectors of the polygon vertices $\boldsymbol{r}_i$ with i being the index of vertices.[1, 2] For simplicity, we assume the properties of each cell are identical. The potential energy of the system is[1]

$$U = \sum_{\alpha} \left[\frac{1}{2} K (A_\alpha - A_0)^2 + \frac{1}{2} \Gamma L_\alpha^2 \right] + \sum_{(i,j)} \Lambda l_{ij} \tag{1}$$

where K, Γ, A_α, and L_α represent the area elastic modulus, contractile modulus, current area, and the perimeter of cell α. A_0 is the reference area of cells in the monolayer. Λ signifies the competition between cell contraction and intercellular adhesion,[3, 4] and l_{ij} represents the length of the intercellular interface ij connecting vertices i and j. In our model, the vertex position $\boldsymbol{r}_i$ can be determined by the overdamped equation

$$\eta \frac{d\boldsymbol{r}_i}{dt} = -\frac{\partial U}{\partial \boldsymbol{r}_i} + \boldsymbol{F}_i^{adhesion} + \boldsymbol{F}_i^{p} + \boldsymbol{F}_i^{\pi} \tag{2}$$

Here, η is the friction coefficient between the cells and the substrate. The right-hand first term in Eq. 2 accounts for the forces due to the system's potential energy gradient.[5] $\boldsymbol{F}_i^{adhesion}$ represents the adhesion force between cells and the substrate. Here, the substrate was modeled as a rigid triangular mesh. The nodes of the triangular mesh are referred to as substrate vertices. We identify the substrate vertices k within the threshold range of each cell vertices i, then $\boldsymbol{F}_i^{adhesion} = \sum_{k=1}^{M} k_{ad} \boldsymbol{r}_{ik}$. Here, M represents the total number of substrate vertices within the threshold range, and k_{ad} represents a force constant.

$\boldsymbol{F}_i^{p}$ and $\boldsymbol{F}_i^{\pi}$ are the hydrostatic pressure and osmotic pressure on cells. Considering that the two forces being vertically applied on the cell surface, we have

$$\boldsymbol{F}_i^{p} = \sum_{\alpha \in C_i} -\frac{p A_\alpha \hat{\boldsymbol{n}}_\alpha}{N_\alpha}, \qquad \boldsymbol{F}_i^{\pi} = \sum_{\alpha \in C_{id}} \frac{\pi A_\alpha \hat{\boldsymbol{n}}_\alpha}{N_\alpha} \tag{3}$$

where p is the hydrostatic pressure per unit area, and π is the osmotic pressure per unit area. C_i represents the cells containing vertex i, and C_{id} represents the dome cells containing vertex i. $\hat{\boldsymbol{n}}_\alpha$ is the unit normal vector of cell α, and the vector points outside of the dome. N_α is the vertex number of cell α.

Calculation of the maximum principal stress

As described previously,[6] the mechanical state of cell α can be characterized by a local stress tensor $\sigma_{\mu\nu}^{\alpha}$ given by

$$\sigma_{\mu\nu}^{\alpha} = -\Pi_\alpha \delta_{\mu\nu} + \frac{1}{2A_\alpha} \sum_{i,j\in\alpha} T_{ij}^{\mu} l_{ij}^{\nu} \tag{4a}$$

$$\Pi_\alpha = -\frac{\partial U}{\partial A_\alpha} = -K(A_\alpha - A_0), \qquad T_{ij} = \frac{\partial U}{\partial l_{ij}} = \Gamma\left(L_\alpha + L_\beta\right) + \Lambda \tag{4b}$$

where Π_α represents the pressure in cell α, $\delta_{\mu\nu}$ is the Kronecker delta function, and T_{ij} represents the tension along the edge-ij, which is shared by cell α and β. μ and ν are the indices of Cartesian components. Therefore, the characteristic equation of the stress tensor can be written as

$$\lambda^3 - I_1\lambda^2 + I_2\lambda - I_3 = 0 \tag{5}$$

where I_1, I_2 and I_3 are principal scalar invariants of the stress tensor. The maximum value of the roots (λ_1, λ_2, and λ_3) of Eq. 5 is the maximum principal stress.

Calculation of the intercellular normal stress

The interactive force on the edge in cell monolayers can be calculated as previously described.[7] For a monolayer with periodic boundary, three cells share a vertex (Fig. S9).

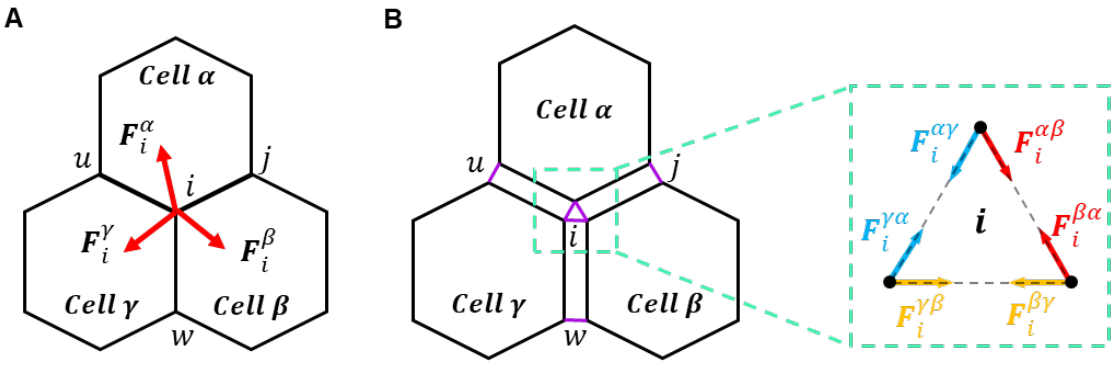

Fig. S9 Illustration of interaction forces at the cell vertex and edge. (A) F_i^α, F_i^β and F_i^γ are the forces exerted by cell α, β, and γ on vertex i. (B) Shared vertex i is virtually subdivided into three virtual vertices, which are connected by chemical bonds. $F_i^{\gamma\beta}$, $F_i^{\beta\alpha}$ and $F_i^{\alpha\gamma}$ are the interactive forces between the virtual vertices.

The forces exerted by cells α, β, and γ on vertex i can be written as

$$\begin{aligned} \boldsymbol{F}_i^\alpha &= \frac{\Pi_\alpha}{2}\left(\hat{\boldsymbol{n}}_{\alpha\gamma} l_{iu} + \hat{\boldsymbol{n}}_{\alpha\beta} l_{ij}\right) + T_\alpha(\hat{\boldsymbol{l}}_{iu} + \hat{\boldsymbol{l}}_{ij}) \\ \boldsymbol{F}_i^\beta &= \frac{\Pi_\beta}{2}\left(\hat{\boldsymbol{n}}_{\beta\alpha} l_{ij} + \hat{\boldsymbol{n}}_{\beta\gamma} l_{iw}\right) + T_\beta(\hat{\boldsymbol{l}}_{ij} + \hat{\boldsymbol{l}}_{iw}) \\ \boldsymbol{F}_i^\gamma &= \frac{\Pi_\gamma}{2}\left(\hat{\boldsymbol{n}}_{\gamma\alpha} l_{iu} + \hat{\boldsymbol{n}}_{\gamma\beta} l_{iw}\right) + T_\gamma(\hat{\boldsymbol{l}}_{iu} + \hat{\boldsymbol{l}}_{iw}) \end{aligned} \quad (6)$$

where the pressure term can be defined as $\Pi_X = -\frac{\partial U_X}{\partial A_X}$, and tension term is $\mathrm{T}_X = \frac{\partial U_X}{\partial L_X}$ $(X = \alpha, \beta, \gamma)$. $\hat{\boldsymbol{n}}_{\alpha\gamma}$ is the unit vector perpendicular to the edge (l_{iu}) shared by cell α and γ. $\hat{\boldsymbol{l}}_{iu}$ is the unit vector of the corresponding edge.

As shown in Fig. S7B, the vertex i can be divided into three virtual vertices connected by chemical bonds. Their interactive forces can be written as

$$\boldsymbol{F}_i^{\gamma\beta} = \frac{1}{3}\left(\boldsymbol{F}_i^\beta - \boldsymbol{F}_i^\gamma\right), \quad \boldsymbol{F}_i^{\beta\alpha} = \frac{1}{3}\left(\boldsymbol{F}_i^\alpha - \boldsymbol{F}_i^\beta\right), \quad \boldsymbol{F}_i^{\alpha\gamma} = \frac{1}{3}(\boldsymbol{F}_i^\gamma - \boldsymbol{F}_i^\alpha) \quad (7)$$

In this way, we can calculate the intercellular force on any edge in the cell monolayer. For example, the intercellular force on edge-ij can be defined as $\boldsymbol{F}_{ij}^{\beta\alpha} = \boldsymbol{F}_i^{\beta\alpha} + \boldsymbol{F}_j^{\beta\alpha}$. The intercellular normal stress can be written as $\sigma_{ij} = F_{ij}^n / l_{ij}$, where F_{ij}^n is the

component of $\boldsymbol{F}_{ij}^{\beta\alpha}$ normal to the edge-ij. Therefore, the larger σ_{ij} is, the more likely the cell monolayer is to break at this edge.

References

1. D. L. Barton, S. Henkes, C. J. Weijer and R. Sknepnek, *PLOS Computational Biology*, 2017, **13**, e1005569.
2. Alexander G. Fletcher, M. Osterfield, Ruth E. Baker and Stanislav Y. Shvartsman, *Biophysical Journal*, 2014, **106**, 2291-2304.
3. R. Farhadifar, J. C. Röper, B. Algouy, S. Eaton and F. Jülicher, *Current Biology*, 2007, **17**, 2095-2104.
4. X. D. Kong, Z. Zhong and C. Fang, *Biophysical Journal*, 2025, **124**, 1995-2004.
5. A. G. Fletcher, J. M. Osborne, P. K. Maini and D. J. Gavaghan, *Progress in Biophysics and Molecular Biology*, 2013, **113**, 299-326.
6. X. B. Yang, D. P. Bi, M. Czajkowski, M. Merkel, M. L. Manning and M. C. Marchetti, *Proceedings of the National Academy of Sciences of the United States of America*, 2017, **114**, 12663-12668.
7. Y. X. Chen, Q. G. Gao, J. C. Li, F. T. Mao, R. W. Tang and H. Y. Jiang, *Physical Review Letters*, 2022, **128**.